Supporting information for

Transition Metal-Doped Ultrathin RuO_2 Networked Nanowires for Efficient Overall Water Splitting in Broad pH Range

Juan Wang,[a#] Yujin Ji,[b#] Rongguan Yin,[b] Youyong Li,[b*] Qi Shao,[a] and Xiaoqing Huang[a*]

[a]College of Chemistry, Chemical Engineering and Materials Science, Soochow University, Jiangsu 215123, China
[b]Institute of Functional Nano & Soft Materials (FUNSOM), Soochow University, Jiangsu 215123, China.
[#]Juan Wang and Yujin Ji contributed equally to this work.
*Email: yyli@suda.edu.cn, hxq006@suda.edu.cn

Experimental Section

Chemicals. Nickel (II) acetate tetrahydrate ($Ni(Ac)_2$, >98%) was purchased from Strem chemicals Inc. Iron (III) acetylacetonate ($Fe(acac)_3$, 97%) and Ruthenium (III) chloride hydrate ($RuCl_3 \cdot xH_2O$, 99.98%) were obtained from Sigma-Aldrich. Cobalt (II) acetate tetrahydrate ($Co(Ac)_2 \cdot 4H_2O$, 99.9%) was available from Aladdin-reagent Inc. Poly (vinylpyrrolidone) (PVP, average M.W. 8000, K15-19) was purchased from J&K Scientific Ltd. Sodium bromide (NaBr, >99), glucose ($C_6H_{12}O_6$, AR), isopropanol (IPA, AR) and ethylene glycol (EG, AR) were available from Sinopharm Chemical Reagent Co. Ltd. (Shanghai, China).

Preparation of Ru NWs and M-doped Ru NWs (M = Fe/Co/Ni). First, 10 mg $RuCl_3 \cdot xH_2O$, 50 mg PVP, 25 mg NaBr and 30 mg $C_6H_{12}O_6$ dispersed in 10 mL EG. The r mixture was maintained at 190 °C about 4 h in an oil bath after ultrasonicated treatment for 30 min. The products were washed by using ethanol/acetone solution. The preparations of Fe-doped Ru NWs, Co-doped Ru NWs and Ni-doped Ru NWs were obtained by adding 5 mg $Fe(acac)_3$, 5 mg $Co(Ac)_2$ and 2 mg $Ni(Ac)_2$ into the mixture, respectively.

Synthesis of M-doped RuO_2 NWs. M-doped Ru NWs were loaded on the Vulcan VCX72 carbon (20wt%, determined by ICP-AES) in 10 mL ethanol with ultrasonicated for 1 h. The resulting homogeneous mixture was washed with ethanol/acetone solution. The powders were annealed at 200 °C for 30 min in air conditions. The products were denoted as RuO_2 NWs, Fe-doped RuO_2 NWs, Co-doped RuO_2 NWs and Ni-doped RuO_2 NWs, respectively.

Characterizations. Transmission electron microscopy (TEM) was performed on a HITACHI HT7700 transmission electron microscope with voltage of 120 kV. High-resolution TEM (HRTEM), scanning transmission electron microscopy energy-dispersive X-ray spectroscopy (STEM-EDS) element mappings and high-angle annular dark-field STEM (HAADF-STEM) were carried out on a FEI Tecnai F20 transmission electron microscope with voltage of 200 kV. Powder X-ray diffraction (PXRD) patterns were collected on a Shimadzu XRD-6000 X-ray diffractometer with a range from 20° to 80° and using a Cu Kα X-ray as source (λ = 1.540598 Å). X-ray photoelectron spectroscopy (XPS) was done with an SSI S-Probe XPS Spectrometer. The concentration of catalyst was determined by the inductively coupled plasma atomic emission spectroscopy (710-ES, Varian, ICP-AES).

Electrochemical measurements. Electrochemical measurements of all samples were performed by using CHI660 electrochemical workstation (Chenhua, Shanghai) with three-electrode system. The glassy carbon (GC), saturated calomel electrode (SCE) and graphite rod were used as working electrode, reference electrode and counter electrode, respectively. For electrochemical measurements, 2 mg catalyst was dispersed in 900 μL IPA, 100 μL H_20 and 10 μL Nafion (5%) with ultrasonication treatment about 0.5h to obtain catalyst ink. Then, 20 μL catalyst ink was deposited on the GC electrode. After that, electrochemical measurements were carried out in 0.5 M H_2SO_4, 0.05 M H_2SO_4, 0.1 M KOH and 1.0 M KOH. All of polarization curves were obtained at the potential range with a scan rate of 5 mV s^{-1} and 95% IR compensation. The long-term stabilities for water were tested by using a two-electrode system.

Computational details. All spin-unrestricted first-principles calculations were ran by using Vienna Ab-initio Simulation Package (VASP) software with the projected augmented wave (PAW).[1,2] The exchange-correlation functional adopts the generalized gradient approximation (GGA) formula proposed by Perdew-Burke- Ernzerhof (PBE) and the convergence standards of energy and force was corresponding to 10^{-4} eV and -0.05 eV/Å, respectively, during self-consistent calculations.[3] The cut-off energy was set about 500 eV. Meanwhile, the empirical Grimme method (DFT-D2) was used to consider weak van der

Waals interaction of HER/OER intermediates into consideration.[4] Besides, the Methfessel-Paxton smearing method with a sigma value 0.05 eV is set to consider the electronic partial occupancies. In the RuO_2 system, the (110) surface of 3 layered RuO_2 is cleaved from its bulk structure (a=3.14 Å, b=c=4.54Å) with a 15 Å vacuum height to avoid the image coupling of periodic boundary condition. The bottom layer is constrained during optimization to simulate the bulk counterpart. The adsorption free energy of G(*H) and G(*OH) is calculated by:

$$G(*H) = E(*H) - E(*) - \frac{1}{2}E(H_2) + \Delta ZPE - T\Delta S$$

$$G(*OH) = E(*OH) - E(*) - (E(H_2O) - \frac{1}{2}E(H_2)) + \Delta ZPE - T\Delta S$$

where E(*OH) and E(*H) are the total energy of substrate after the adsorption of H and OH. E(*) is the total energy of substrate without adsorption of intermediates. $E(H_2O)$ and $E(H_2)$ are the total energy of H_2O and H_2 in gas phase. ΔZPE is the zero-point energy based on finite differences method and the ΔS is the contribution of entropy.

Supporting Figures and Tables.

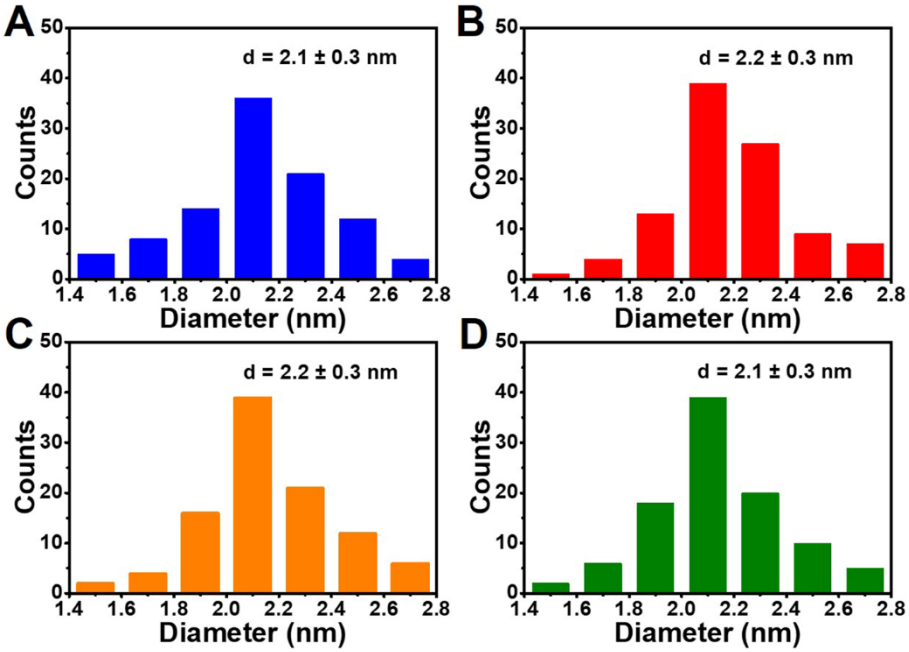

Fig. S1 Size distributions of (a) Co-doped Ru NWs, (b) Ni-doped Ru NWs, (c) Fe-doped Ru NWs and (d) Ru NWs.

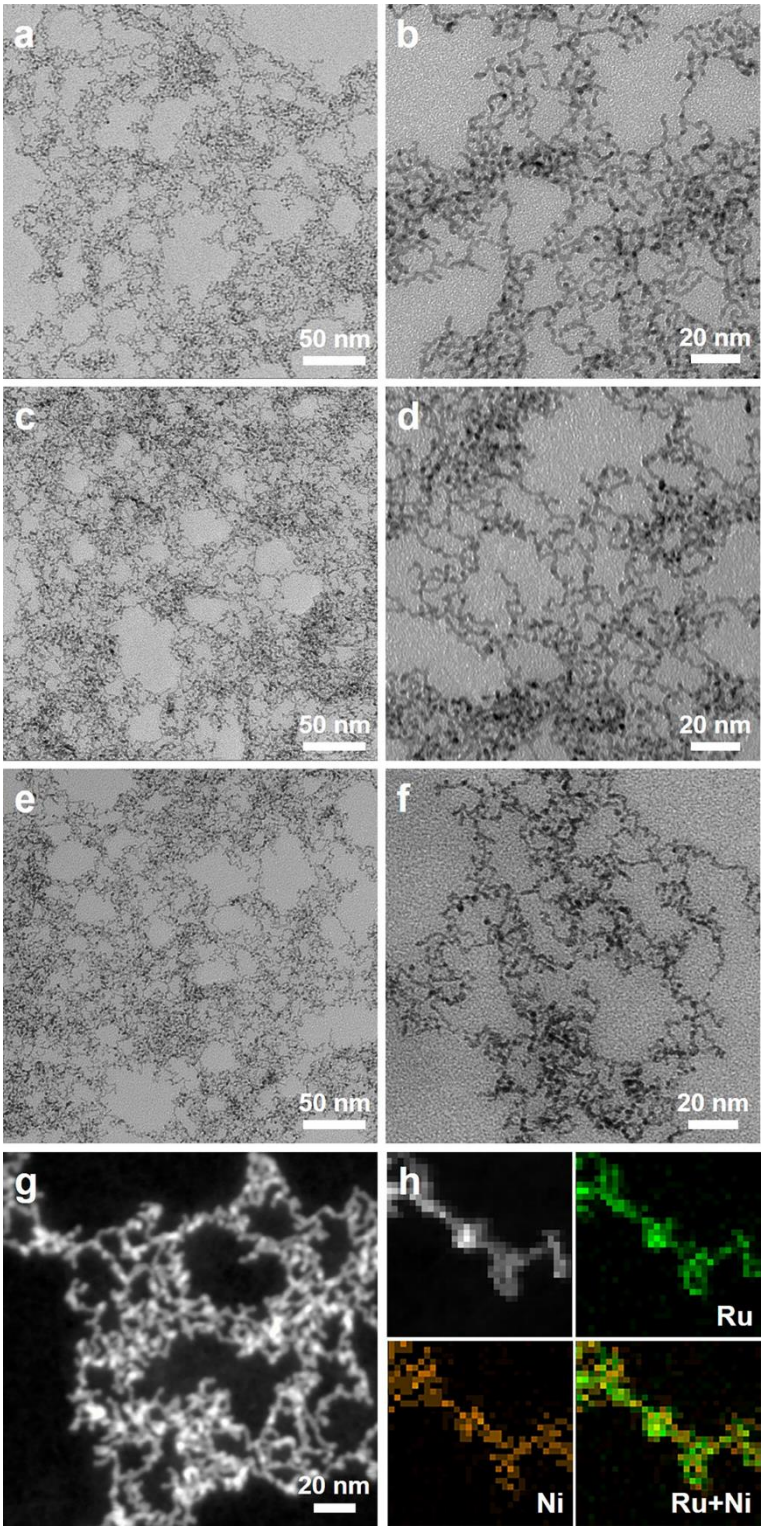

Fig. S2 TEM images of (a, b) Ru NWs, (c, d) Fe-doped Ru NWs and (e, f) Ni-doped Ru NWs. (g) HADDF-STEM image and (h) STEM-EDS element mappings of Ni-doped Ru NWs.

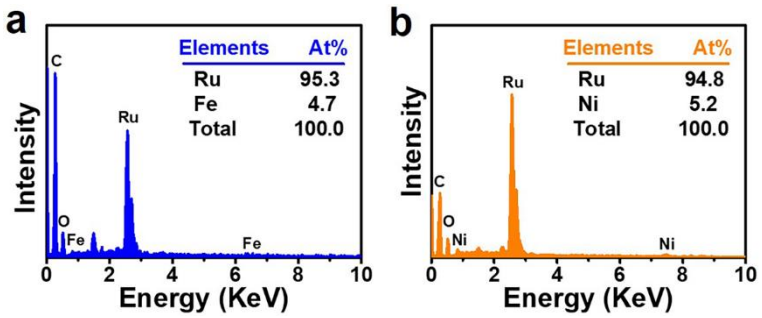

Fig. S3 SEM-EDS spectra of (a) Fe-doped Ru NWs and (b) Ni-doped Ru NWs.

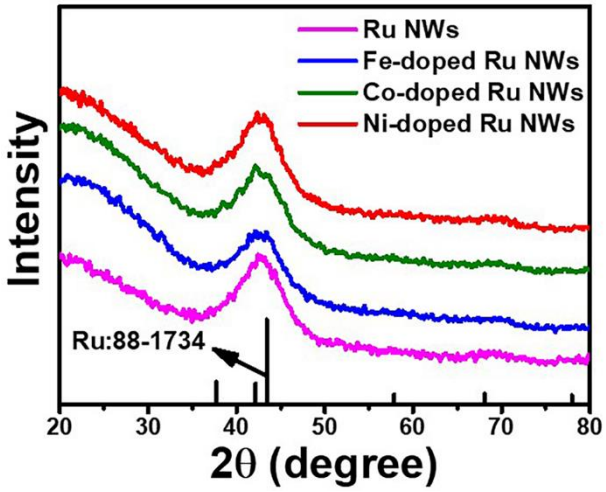

Fig. S4 PXRD patterns of M-doped Ru NWs.

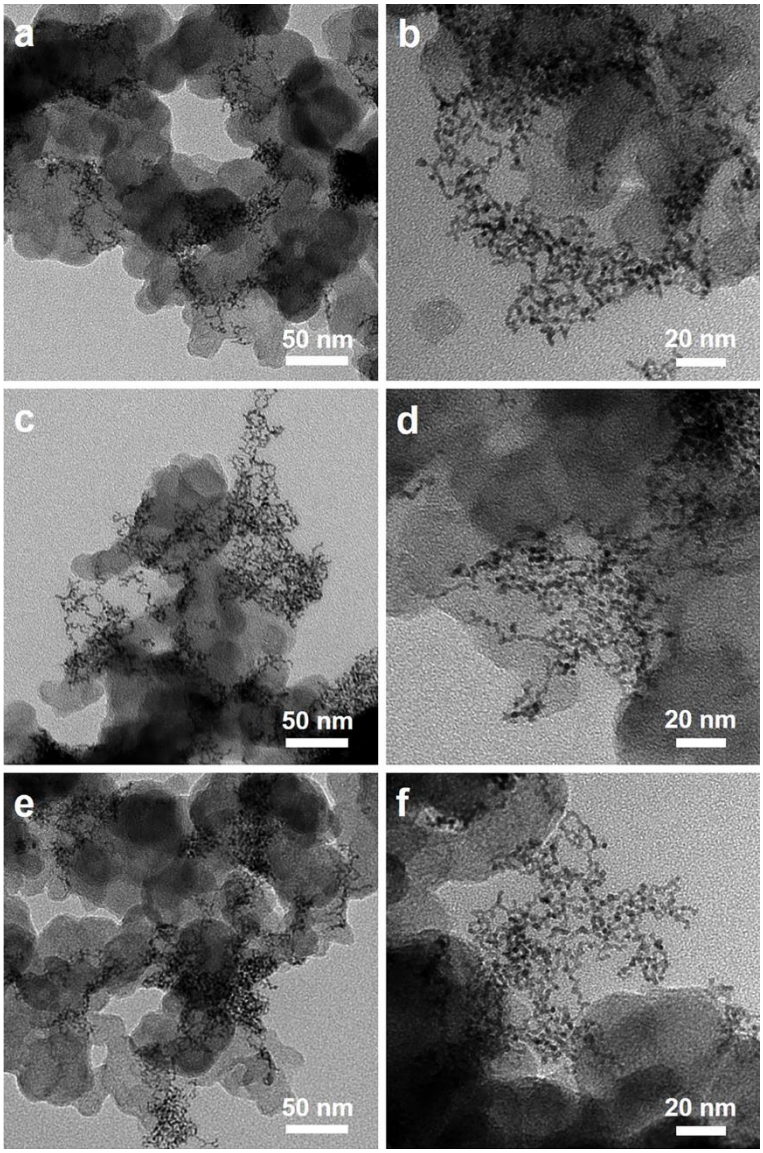

Fig. S5 TEM images of carbon supported (a, b) RuO_2 NWs, (c, d) Fe-doped RuO_2 NWs and (e, f) Ni-doped RuO_2 NWs.

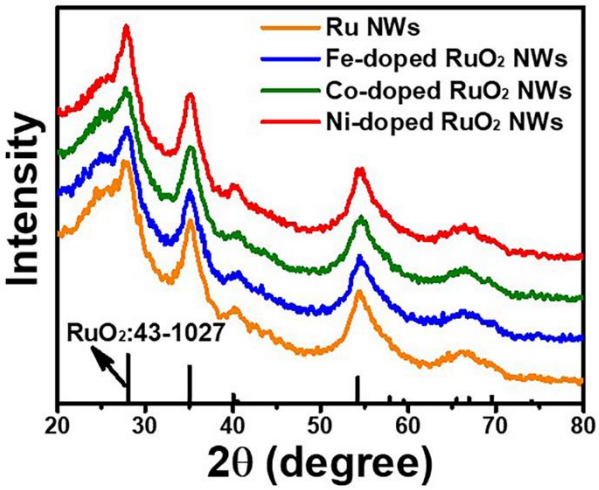

Fig. S6 PXRD patterns of M-doped RuO_2 NWs.

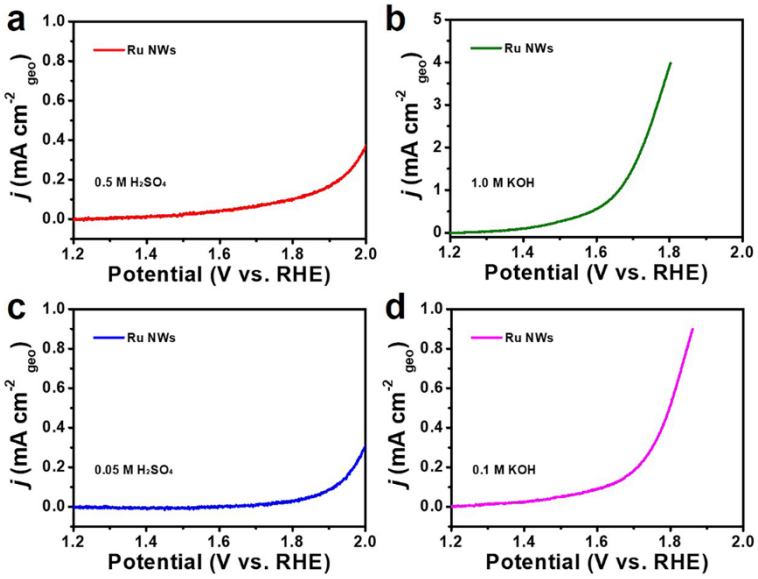

Fig. S7 OER polarization curves of Ru NWs in (a) 0.5 M H_2SO_4, (b) 1.0 M KOH, (c) 0.05 M H_2SO_4 and (d) 0.1 M KOH.

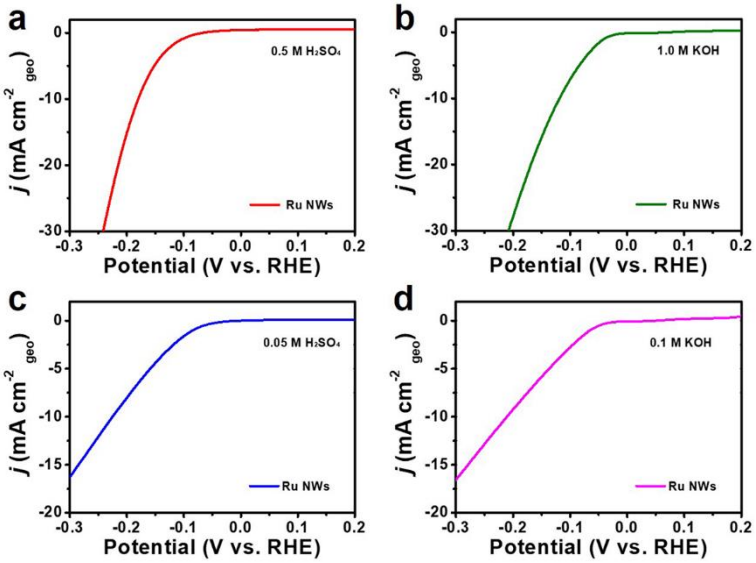

Fig. S8 HER polarization curves of Ru NWs in (a) 0.5 M H_2SO_4, (b) 1.0 M KOH, (c) 0.05 M H_2SO_4 and (d) 0.1 M KOH.

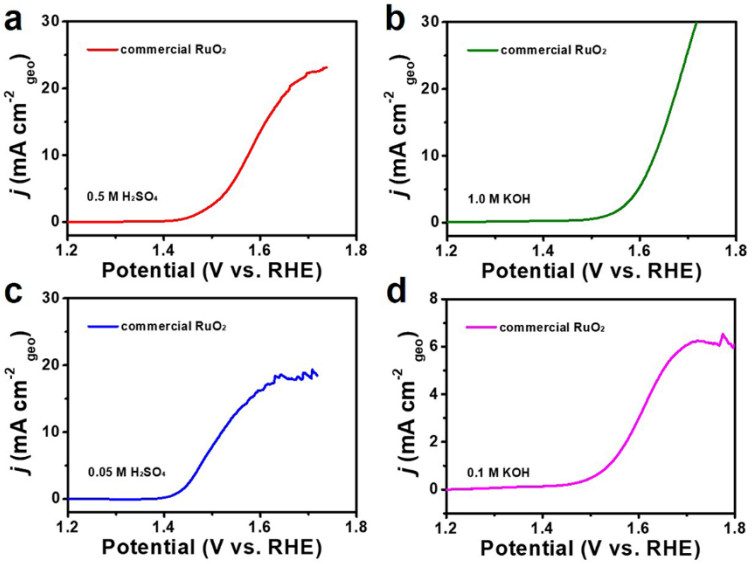

Fig. S9 OER polarization curves of commercial RuO_2 in (a) 0.5 M H_2SO_4, (b) 1.0 M KOH, (c) 0.05 M H_2SO_4 and (d) 0.1 M KOH.

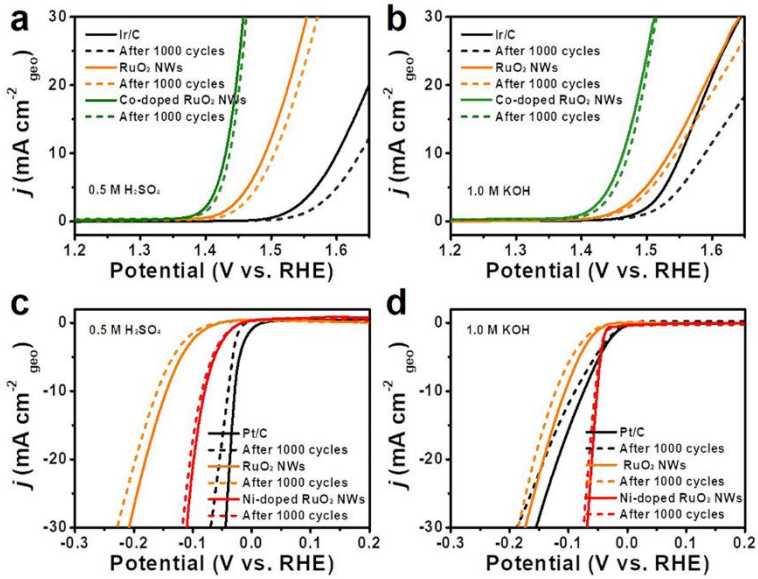

Fig. S10 OER polarization curves of commercial Ir/C, RuO_2 NWs and Co-doped RuO_2 NWs in (a) 0.5 M H_2SO_4 and (b) 1.0 M KOH. HER polarization curves of commercial Pt/C, RuO_2 NWs and Ni-doped RuO_2 NWs in (c) 0.5 M H_2SO_4 and (d) 1.0 M KOH. The solid line is the 1st cycle and the dotted line is the 1000th cycle.

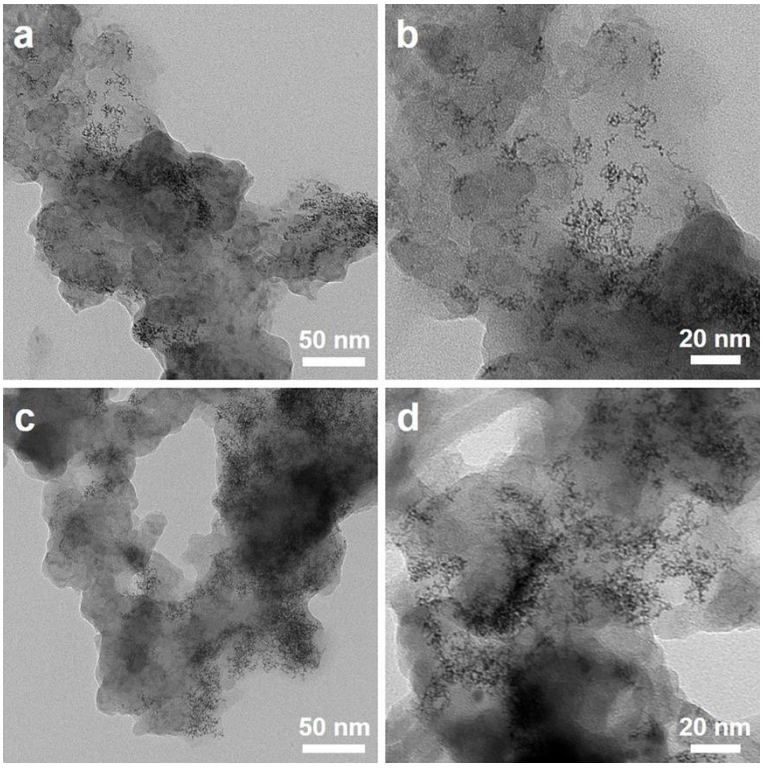

Fig. S11 TEM images of carbon supported (a, b) Co-doped RuO_2 NWs and (c, d) Ni-doped RuO_2 NWs after water splitting in 0.5 M H_2SO_4.

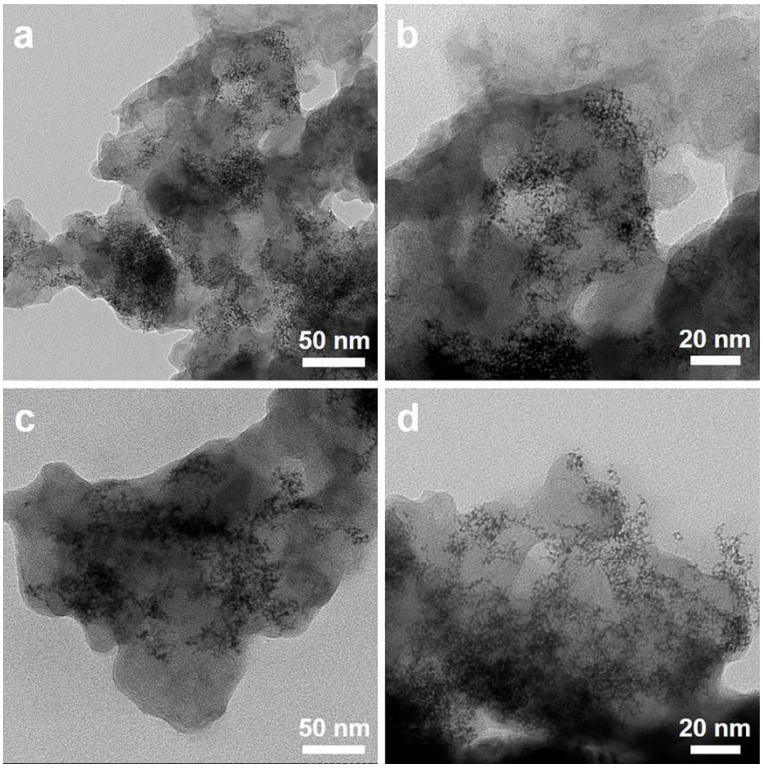

Fig. S12 TEM images of carbon supported (a, b) Co-doped RuO_2 NWs and (c, d) Ni-doped RuO_2 NWs after water splitting in 1.0 M KOH.

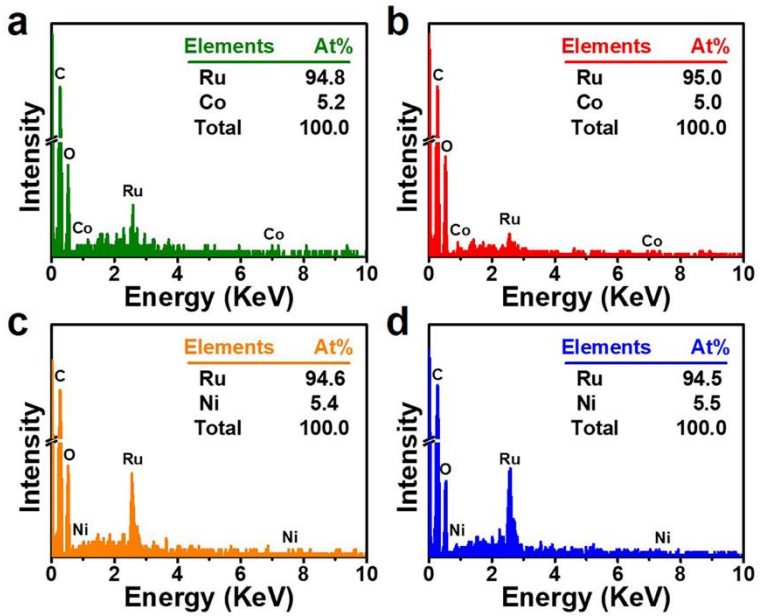

Fig. S13 SEM-EDS spectra of Co-doped RuO_2 NWs after water splitting in (a) 0.5 M H_2SO_4 and (b) 1.0 M KOH. SEM-EDS spectra of Ni-doped RuO_2 NWs after water splitting in (c) 0.5 M H_2SO_4 and (d) 1.0 M KOH.

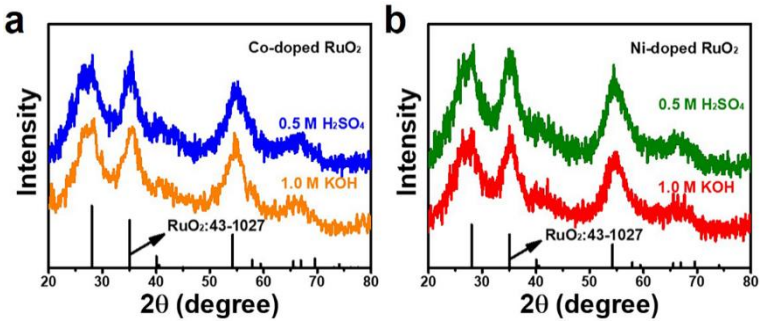

Fig. S14 PXRD patterns of Co-doped RuO_2 NWs after water splitting in (a) 0.5 M H_2SO_4 and 1.0 M KOH and Ni-doped RuO_2 NWs after water splitting in (b) 0.5 M H_2SO_4 and 1.0 M KOH.

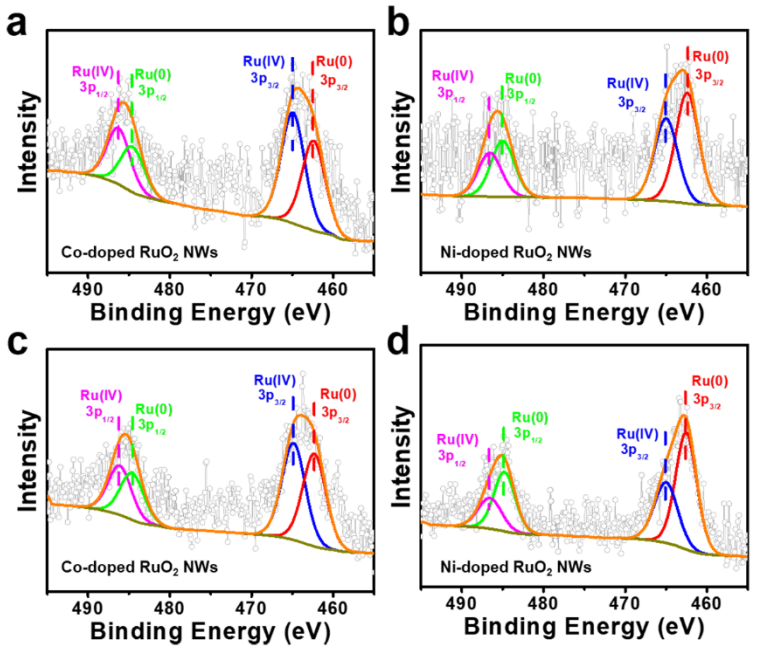

Fig. S15 Ru 3p XPS spectra of (a) Co-doped RuO_2 NWs and (b) Ni-doped RuO_2 NWs after water splitting in 0.5 M H_2SO_4. Ru 3p XPS spectra of (c) Co-doped RuO_2 NWs and (d) Ni-doped RuO_2 NWs after water splitting in 1.0 M KOH.

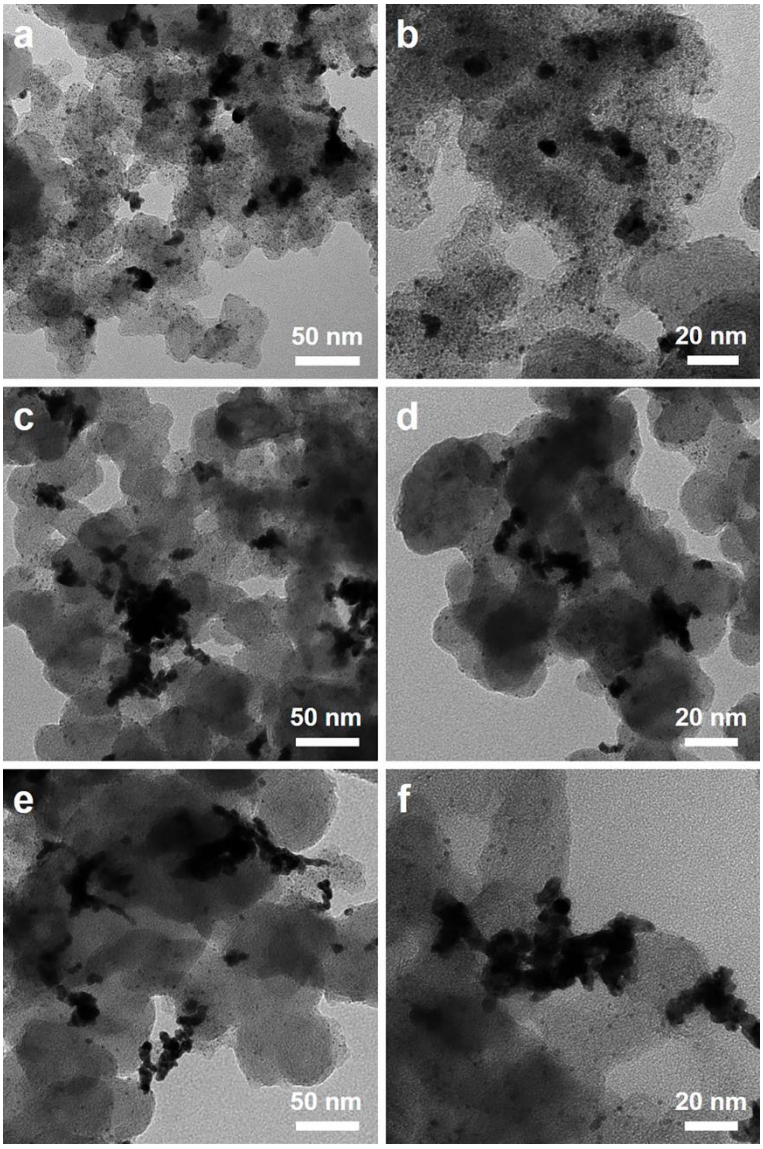

Fig. S16 TEM images of commercial Ir/C (a, b) before water splitting. TEM images of commercial Ir/C after water splitting in (c, d) 0.5 M H_2SO_4 and (e, f) 1.0 M KOH.

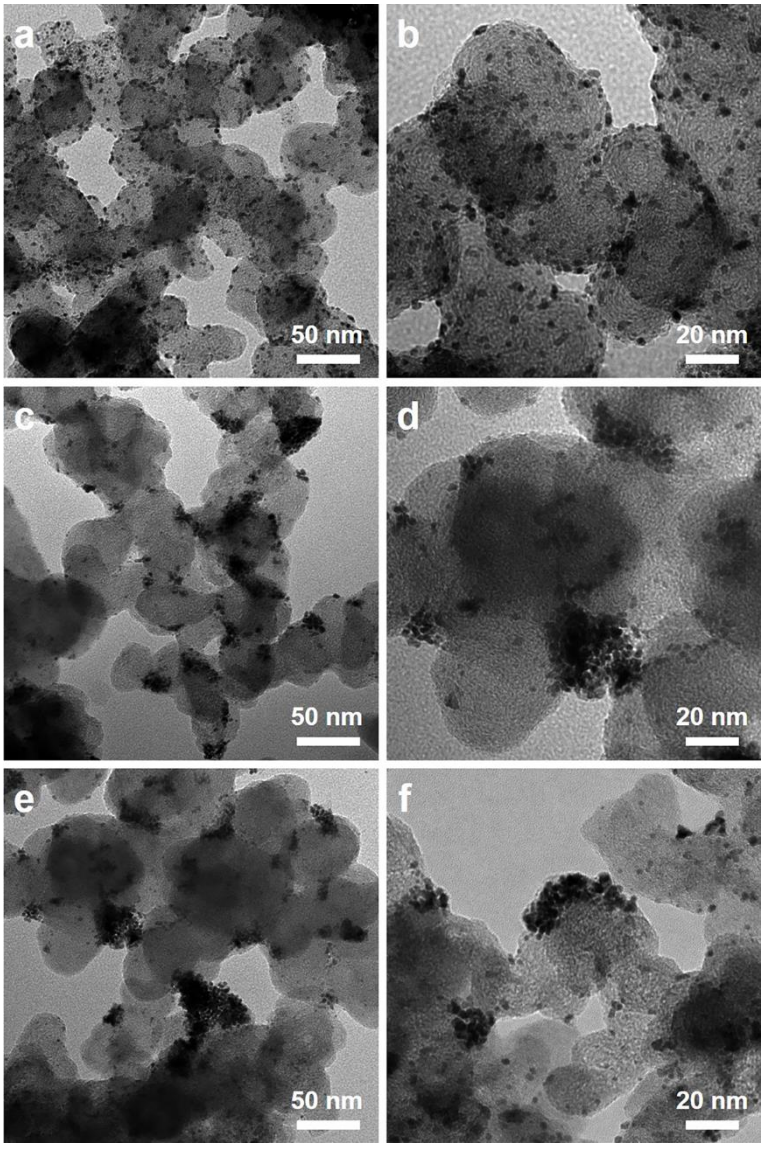

Fig. S17 TEM images of commercial Pt/C (a, b) before water splitting. TEM images of commercial Pt/C after water splitting in (c, d) 0.5 M H_2SO_4 and (e, f) 1.0 M KOH.

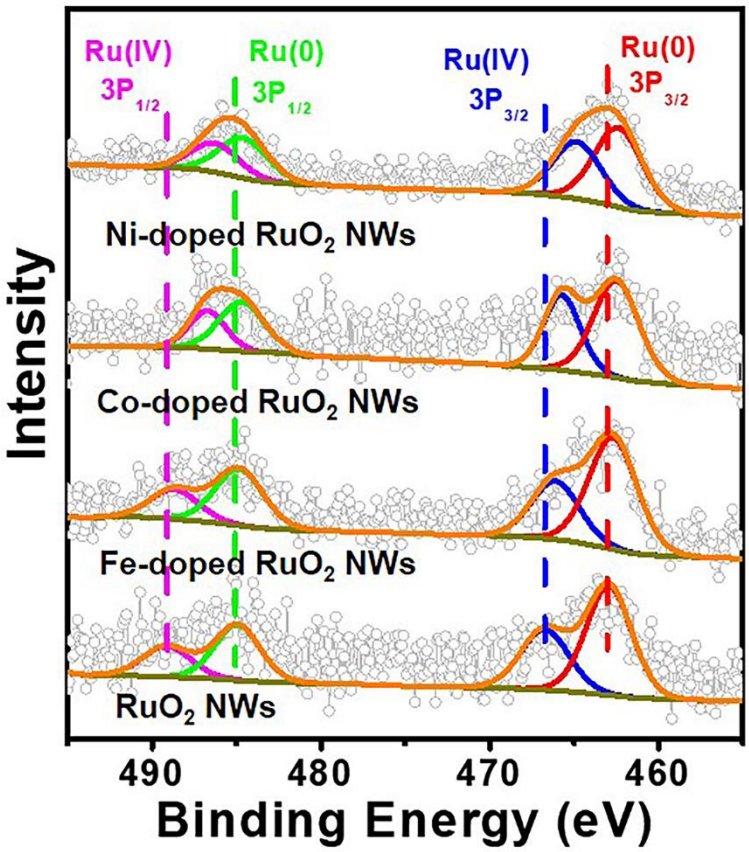

Fig. S18 XPS spectra of Ru 3p of M-doped RuO_2 NWs.

Table S1 Summary of recently reported OER electrocatalysts in different electrolytes.

Catalyst	Electrolyte	Current density	Overpotential (mV)	Reference
Co-doped RuO_2 NWs	**0.5 M H_2SO_4**	**10 mA cm^{-2}**	**200**	**This work**
Rh_2P/C	0.5 M H_2SO_4	5 mA cm^{-2}	510	*J. Am. Chem. Soc.* **139**, 5494-5502 (2017).
$ZnFe_{0.4}Co_{1.6}O_4$	1.0 M KOH	10 mA cm^{-2}	~340	*Adv. Mater.* DOI: 10.1002/adma.201802912.
Au@Ir NRB	0.5 M H_2SO_4	10 mA cm^{-2}	296	*Small* **12**, 3908-3913 (2016).
HG-NiFe	1.0 M KOH	10 mA cm^{-2}	310	*Sci. Adv.* **4**, eaap7970 (2018).
CFP/$NiCo_2O_4$/ $CoO_{0.53}Ni_{0.47}$LMOs	0.1 M KOH	10 mA cm^{-2}	34	*Nanoscale* **8**, 1390-1400 (2016).
PdNi/CNFs-1:2	1.0 M KOH	10 mA cm^{-2}	289	*Electrochim. Acta* **246**, 17-26 (2017).
Co_3O_4	0.1 M KOH	10 mA cm^{-2}	~320	*J. Am. Chem. Soc.* **138**, 36-39 (2016).
Fe/P/C	1.0 M KOH	10 mA cm^{-2}	330	*Nano Energy* **33**, 221-228 (2017).

Table S2 Summary of recently reported HER electrocatalysts in different electrolytes.

Catalyst	Electrolyte	Current density	Overpotential (mV)	Reference
Ni-doped RuO_2 NWs	**1.0 M KOH**	**10 mA cm^{-2}**	**52**	**This work**
Li-PPS NDs	0.5 M H_2SO_4	10 mA cm^{-2}	91	*Nat. Catal.* **1**, 460-468 (2018).
$Ru/C_3N_4/C$	0.5 M H_2SO_4	10 mA cm^{-2}	79	*J. Am. Chem. Soc.* **138**, 16174-16181 (2016).
Pt_3Ni_3 NWs	0.05 M H_2SO_4	5 mA cm^{-2}	60	*Angew. Chem. Int. Ed.* **128**, 13051-13055 (2016).
FeP|S-5mg	0.5 M H_2SO_4	10 mA cm^{-2}	74	*ACS Catal.* **7**, 4026-4032 (2017).
Au@CoP	0.5 M H_2SO_4	1 mA cm^{-2}	160	*Nano Energy* **50**, 273-280 (2018).
$3DGN/IrO_2$	1.0 M KOH	10 mA cm^{-2}	277	*Adv. Mater*. **28**, 7640-7645 (2016).
FeP NWs/rGO	0.5 M H_2SO_4	10 mA cm^{-2}	107	*Adv. Sci.* **2**, 1500120 (2015).
Au-Cu/CNFs-1:2	0.5 M H_2SO_4	10 mA cm^{-2}	83	*ACS Appl. Mater. Interfaces* **9**, 19756-19765 (2017).

Table S3 Summary of recently reported overall water splitting electrocatalysts in different electrolytes.

Catalyst	Electrolyte	Current density	Potential (V)	Reference
Co-doped RuO_2 NWs ||Ni-doped RuO_2 NWs	**0.5 M H_2SO_4**	**10 mA cm^{-2}**	**1.537**	**This work**
	1.0 M KOH	**10 mA cm^{-2}**	**1.542**	
Ru_2Ni_2 SNs/C ||Ru_2Ni_2 SNs/C	1.0 M KOH	10 mA cm^{-2}	1.58	*Nano Energy* **47**, 1-7 (2018).
IrNi NCs||IrNi NCs	0.5 M H_2SO_4	10 mA cm^{-2}	1.58	*Adv. Funct. Mater.* **27**, 1700886 (2017).
RuO_2/NiO/CF ||RuO_2/NiO/CF	1.0 M KOH	10 mA cm^{-2}	1.50	*Small* **14**, 1704073 (2018).
IrCoNi CFP ||IrCoNi CFP	0.5 M H_2SO_4	2 mA cm^{-2}	1.56	*Adv. Mater.* **29**, 1703798 (2017).
CFP/$NiCo_2O_4$ ||CFP/$NiCo_2O_4$	0.5 M H_2SO_4	18 mA cm^{-2}	1.5	*Adv. Funct. Mater.* **25**, 6814-6822 (2015).
CoP/NCNHP ||CoP/NCNHP	1.0 M KOH	10 mA cm^{-2}	1.64	*J. Am. Chem. Soc.* **140**, 2610-2618 (2018).
NiS_2/CoS_2||NiS_2/CoS_2	1.0 M KOH	10 mA cm^{-2}	1.78	*Adv. Mater.* **29**, 1704681 (2017).
Co_3O_4-MTA ||Co_3O_4-MTA	1.0 M KOH	10 mA cm^{-2}	1.53	*Angew. Chem. Int. Ed.* **56**, 1324-1328 (2017).

Notes and references

1 G. Kresse, J. Furthmüller, *Phys. Rev. B* 1996, **54**, 11169.
2 P. E. Blöchl, *Phys. Rev. B* 1994, **50**, 17953.
3 J. P. Perdew, K. Burke, M. Ernzerhof, *Phys. Rev. Lett.* 1996, **77**, 3865.
4 S. Grimme, *J. Comput. Chem*, 2006, **27**, 1787.